HHS Public Access

Author manuscript

J Magn Reson. Author manuscript; available in PMC 2016 June 01.

Published in final edited form as:

J Magn Reson. 2015 June ; 255: 68–76. doi:10.1016/j.jmr.2015.03.014.

Spin-Label CW Microwave Power Saturation and Rapid Passage with Triangular Non-Adiabatic Rapid Sweep (NARS) and Adiabatic Rapid Passage (ARP) EPR Spectroscopy

Aaron W. Kittell and **James S. Hyde***

National Biomedical EPR Center, Department of Biophysics, Medical College of Wisconsin, 8701 Watertown Plank Road, Milwaukee, WI 53226 USA

Abstract

Non-adiabatic rapid passage (NARS) electron paramagnetic resonance (EPR) spectroscopy was introduced by Kittell, A.W., Camenisch, T.G., Ratke, J.J. Sidabras, J.W., Hyde, J.S., 2011 as a general purpose technique to collect the pure absorption response. The technique has been used to improve sensitivity relative to sinusoidal magnetic field modulation, increase the range of inter-spin distances that can be measured under near physiological conditions, and enhance spectral resolution in copper (II) spectra. In the present work, the method is extended to CW microwave power saturation of spin-labeled T4 Lysozyme (T4L). As in the cited papers, rapid triangular sweep of the polarizing magnetic field was superimposed on slow sweep across the spectrum. Adiabatic rapid passage (ARP) effects were encountered in samples undergoing very slow rotational diffusion as the triangular magnetic field sweep rate was increased. The paper reports results of variation of experimental parameters at the interface of adiabatic and non-adiabatic rapid sweep conditions. Comparison of the forward (up) and reverse (down) triangular sweeps is shown to be a good indicator of the presence of rapid passage effects. Spectral turning points can be distinguished from spectral regions between turning points in two ways: differential microwave power saturation and differential passage effects. Oxygen accessibility data are shown under NARS conditions that appear similar to conventional field modulation data. However, the sensitivity is much higher, permitting, in principle, experiments at substantially lower protein concentrations. Spectral displays were obtained that appear sensitive to rotational diffusion in the range of rotational correlation times of 10^{-3} to 10^{-7} s in a manner that is analogous to saturation transfer spectroscopy.

Keywords

Nitroxide; Spin-label; NARS; EPR; Adiabatic Rapid Passage; Oxygen Accessibility; Paramagnetic Ion Accessibility; Power Saturation; Saturation Transfer

*Corresponding author: James S. Hyde jshyde@mcw.edu 8701 Watertown Plank Road, Milwaukee, WI, 53226 USA 414-955-4308.

1. Introduction

1.1 Background for Non-Adiabatic Rapid Sweep (NARS) Electron Paramagnetic Resonance (EPR) Spectroscopy

Electron paramagnetic resonance (EPR) spectroscopy in combination with site-directed mutagenesis and spin-labeling can be used to study the structure and dynamics of biologically relevant proteins [1]. Although there are numerous EPR techniques available, it has become standard to investigate spin-labeled proteins by analyzing the continuous wave (CW) EPR spectrum.

Historically, CW EPR spectra have been collected by holding the microwave frequency constant and slowly sweeping a sinusoidally modulated magnetic field through the resonance condition. The signal is detected by collecting the first harmonic response with a phase-sensitive detector (PSD) set to the modulating frequency. Although this detection scheme improves baseline stability and overcomes $1/f$ noise, it carries a trade-off between signal height and spectral resolution as a function of the modulation amplitude.

The drawbacks associated with magnetic field modulation are well documented [2, 3], and a number of alternative detection schemes have been developed to address some of those problems [4-6]. More recently, Hyde and co-workers developed Non-Adiabatic Rapid Sweep (NARS) EPR to overcome the drawbacks associated with field modulation [7]. In NARS, the polarizing magnetic field consists of the static magnetic field H_0, which is stepped slowly in time, plus a time-varying triangular magnetic field. Both fields must be homogeneous over the sample. The intent of the method is that the triangular sweep be sufficiently slow that the spins respond in the same manner as they would if only a slowly varying H_0 were present. The triangular sweep frequency is set at a value that is sufficiently high that $1/f$ noise is overcome. The full spectrum is obtained by collecting successive segments in a digital signal averager, followed by alignment and summation of overlapping spectral components. A pure absorption spectrum is obtained rather than the derivative-like spectrum that is conventionally acquired when using sinusoidal field modulation and phase-sensitive detection.

NARS provides several advantages over sinusoidal magnetic field modulation. Perhaps the greatest benefit, which results from time-averaging and collection of the pure absorption, is an improvement in sensitivity by a factor of four or more [7]. Collection of the pure absorption also avoids the line-shape–line-height compromise associated with field modulation. This enabled measurement of inter-spin distances at L-band [8] where linewidths are typically as narrow as one Gauss. Use of small modulation amplitudes in conventional EPR to ensure high spectral resolution resulted in insufficient signal amplitude to make this measurement. In addition, post-processing can be applied to the pure absorption spectrum to obtain the display of choice. In copper (II) spectra, the Moving Difference (MDIFF) algorithm was applied to the pure absorption spectrum to enhance the resolution of selected spectral features in a finite-difference display [9].

1.2 NARS Spectroscopy Under Conditions of CW Microwave Power Saturation

When using NARS with segmental acquisition, the CW microwave power saturation spectrum consists of the response of each point in the spectrum to increasing microwave power. There is no blurring of the saturation response as occurs from the use of magnetic field modulation in ordinary microwave power saturation experiments. For example, if one had a single homogeneously broadened line, the ordinary CW EPR spectrum when using field modulation under saturation conditions would be the off-resonance responses at the peaks of the derivative-like line, whereas in NARS it would be the response at the center of the EPR absorption line. The CW saturation response would be expected to be different in these two situations.

In the present work, we utilize NARS to investigate the saturation behavior of a spin-label attached to a slowly tumbling protein. Saturation studies have commonly been performed by measuring the peak-to-peak line height of the center line of the field modulated first harmonic as a function of the incident microwave power [10]. Structural information is obtained by observing the changes in this relationship in the presence of various paramagnetic relaxation enhancers.

We have discovered an interesting range of conditions in the very slow tumbling range of rotational correlation times where the turning points saturate differently from the regions between turning points. It is presumed that this effect arises from the spectral variation of the effective T_2 value. In this way, the turning points, which are characterized by slow anisotropic rotational diffusion in a defined solid angle, are revealed.

This is a new result.

1.3 Experiments Conducted at the Transition Between Non-Adiabatic Rapid Sweep and Adiabatic Rapid Passage

The ability to study the role of the sweep direction also makes NARS suitable for investigating the onset of adiabatic rapid passage effects. There does not seem to be any prior experimental literature exploring the field of EPR spectroscopy at the interface of adiabatic and non-adiabatic sweeps of the polarizing magnetic field. The presence of passage effects in NARS spectroscopy is observed as a shift of spectral intensity in the direction of the sweep, whether up or down. This is the direction in which free induction decay (FID) signals are observed [5]. This phenomenon also occurs when detecting the dispersion using sinusoidal magnetic field modulation. Shifts of spectral intensity result in a change in phase of the signal [11, 12]. A critical test of the presence of passage effects in NARS is reported here. If “up-field sweep” and “down-field sweep” pure absorption spectra are obtained (see Fig. 1) and displayed as a sweep in the same direction, then the spectra are substantially identical in the absence of passage effects. Another critical test is provided by the g-value moment theorem of Hyde and Pilbrow [13]. The theorem states that at the spectral point of the absorption rigid limit spectrum where the first moment is zero, the point corresponds to the trace of the g-tensor. Shifts of intensity due to passage lead to failure of the theorem.

Hyde and Dalton [14] observed that a range of conditions of very long rotational correlation time of a nitroxide spin label exists when the spectrum is substantially identical to that of a powder at low power but shows unusual passage effects at high power when using 100 kHz field modulation. They established that passage effects occur at the spectral turning points of the anisotropic Zeeman and hyperfine coupling but to a lesser degree at spectral points between turning points. This method is known as saturation transfer EPR spectroscopy (ST-EPR). It has been extensively used to study slow rotational diffusion. Reviews were provided by Beth [15] and by Marsh [16].

The use of sinusoidal modulation complicates the study of passage effects including ST-EPR. Weger described eleven different cases of passage and the various conditions where they apply [17]. Each case is determined by the incident microwave power, the relaxation properties of the spin system, and the spectral sweep rate. The superposition of a sinusoid on to the field sweep produces a non-uniform sweep rate, where the maximum rate is encountered at the zero crossover of the sinusoid and goes to zero at the extremities. This can create mixed states of passage within the modulation cycle, particularly at high incident powers. The combination of these passage states will be reflected in the line shape.

Passage effects in the NARS display offer an opportunity to advance this line of research, and this work provides an overview of this opportunity. The main advantages are: i) that the sweep rate does not vary over the sweep cycle except for a change in sign, ii) that the sweep rate can be precisely adjusted by changing the triangular sweep amplitude, and iii) that data are obtained at a spectral point rather than summed in a complicated manner across the customary 5G field modulation amplitude.

NARS provides an opportunity to study both saturation and passage effects by adjustment of the incident microwave power and the parameters of the triangular sweep. The present study shows how the onset of saturation is altered across the spectrum when the rate and direction of the NARS sweep is varied. The results show that NARS is a natural approach to investigate CW microwave power saturation, assess the validity of line shape models, and exploit passage effects to study saturation transfer.

2. Methods

2.1 Sample Preparation

A single mutant of T4 Lysozyme (T4L) with a cysteine residue inserted at position 68 was expressed, purified, and spin-labeled as described previously [18]. The plasmid was kindly provided by Dr. Wayne Hubbell (University of California, Los Angeles) and was labeled in a ten-fold molar excess of deuterated (1-2,2,5,5,-tetramethylpyrroline-3-methyl) methanethiosulfonate spin-label (pdMTSL, Toronto Research Chemicals, Toronto, ON, Canada). Deuterated spin-labels were used to reduce inhomogeneous broadening resulting from residual superhyperfine structure, but this is not essential to the success of the methods presented. Excess label was removed using a HiPrepTM 26/10 desalting column (GE Healthcare) and was concentrated to approximately 500 μM before adding deuterated glycerol (50% v/v), yielding a final protein concentration of 250 μM. Similar to the deuteration of the spin-label, deuterated solvents were used to reduce linewidths, but are not

essential to the success of the methods discussed. The sample solution was placed in a 0.6 mm ID gas permeable TPX tube sealed at one end.

2.2 EPR Spectroscopy

CW and NARS spectra were collected using a Varian E-9 spectrometer fitted with a modified X-band bridge (~9.35 GHz). The bridge was equipped with a two-loop–one-gap ceramic, silver plated 1 mm ID resonator with a loaded Q of approximately 600 and a measured Λ of 4.7 $G/W^{1/2}$ (Molecular Specialties, Milwaukee, WI).

Unless otherwise noted, samples were degassed via nitrogen flow for 20 minutes at room temperature prior to adjusting to the recording temperature. By removing molecular oxygen from the system, less microwave power is required to saturate the system. Temperature control was achieved with a modified Varian V6050 variable temperature control unit equipped with an Omega (Stamford, CT) microprocessor and gas exchange system.

Conventional CW EPR spectra were collected using 100 kHz magnetic field modulation with an amplitude of 1.2 G. Four, one minute 146 G scans were collected at powers ranging from 0.05-35 mW using an in-house LabVIEW® data acquisition program (4096 points, 32 ms time constant). All spectra were baseline corrected and then smoothed with a five-point Savitzky- Golay filter.

The NARS experiment has been described previously [7]. Unless otherwise specified, spectra were collected using a 5.2 kHz triangular sweep with amplitudes ranging from 2.5 to 25 Gauss. The resonance profile was collected stepwise, moving the field approximately $1/25^{th}$ of the triangular amplitude after each successive collection, acquiring a maximum of 50k averages per segment. The preferred method to construct the pure absorption has been discussed previously [9]; it consists of aligning common portions of successive segments and adding those pieces together sequentially using an in-house software program. This technique is sometimes referred to as string concatenation with overlap. Here, it will be referred to as NARS segmental overlap. All spectra were constructed using 15 segments of overlap regardless of step size. Constructed NARS spectra were baseline corrected with a third order polynomial, interpolated to 4096 points, and smoothed with a five point Savitzky-Golay filter.

CW and NARS spectra were collected consecutively without changes in power or microwave bridge tuning. All spectra from a single temperature point were collected on the same day. Some experiments were repeated on different days to assess sample stability and were found to be in good agreement with previous spectral acquisitions.

2.3 Post-Processing

In instances where CW and NARS spectra are compared, additional post-processing is required. If the comparison of the pure absorption is desired, CW spectra are integrated. If comparison of the first harmonic is desired, the first harmonic of the NARS spectrum is calculated using the MDIFF algorithm set to the desired field modulation amplitude [9]. In cases where the CW and NARS intensities are compared, the raw NARS and CW signal

amplitudes at low microwave power were used to scale results at higher incident power levels.

2.4 Power Saturation

Saturation curves were calculated by fitting data to Eq. 1, where A is the intensity of the

$$A = IP^{1/2}\left[\frac{1+\left(2^{1/\varepsilon}-1\right)P}{P_{1/2}}\right]^{-\varepsilon} \quad (1)$$

central peak of the NARS spectrum or the integrated CW spectrum, I is a scaling factor, P is the incident microwave power, $P_{1/2}$ is the power at which the intensity of the center line is half of its unsaturated intensity, and ε is a line homogeneity factor [19].

3. Results

3.1 Saturation Behavior

CW and NARS EPR spectra of T4L-68 were collected at three temperatures and at ten different incident microwave powers. Figure 2 displays the power saturation curves of each technique comparing the peak-to-peak line height of the center line in the field modulated first harmonic to the central peak intensity of the NARS pure absorption (260 kG/s). For display purposes, NARS intensities were scaled so that the peak-to-peak CW intensity and central peak intensity of the NARS spectrum were equal at the lowest microwave power. All subsequent NARS intensities were scaled by this calculated constant. In the case of Fig. 2, the sweep rates of the field modulation cycle and the triangular sweep were similar. As a result, the two sets of saturation curves show little difference (<8% difference $P_{1/2}$ values), establishing that NARS is a suitable technique for power saturation studies. The advantage of using NARS in such studies is an improvement in sensitivity [7].

Figure 3 displays an example of an oxygen accessibility experiment using both the CW and NARS techniques. The $\Delta P_{1/2}$ values were observed to be 0.43 mW for NARS and 0.70 mW for CW. Although the turning points are enhanced in the first harmonic display, the intensities of the high and low-field manifolds between turning points in the NARS display are sensitive to oxygen accessibility. Consequently, oxygen accessibility can be assessed at multiple spectral positions in the NARS experiment.

Figure 4 provides additional information on differences in saturation observed when comparing NARS and CW saturation under various rotational diffusion conditions. Minimal differences are observed between the two techniques at low powers, as shown in the first column, which is in agreement with previous work [7]. However, at moderate saturating microwave powers (Columns 2 and 3), NARS spectra are narrower, less intense, and have more inflections. Furthermore, these characteristic differences increase as the temperature decreases, signifying that some of this effect is related to rotational diffusion. The largest variation is observed in the central feature, where the three components of the g-tensor appear to saturate differently in the two techniques. The cause for the variation across all nuclear quantum number manifolds in Fig. 4 lies in the fact that the NARS spectra in regions

between turning points are more difficult to saturate in the NARS display. These regions tend to be of low intensity in the CW derivative display and do not contribute as much to the integrated spectrum.

At the lowest power and the highest temperature, it is apparent that motional narrowing has started to occur. The outside wings are shifted and broadened, and these regions saturate less readily than the intense central feature. We attribute this to the effects of T_2, since T_1 changes very little throughout the spectrum. As motion is decreased, the difference in T_2 across the spectrum is less noticeable because rotational diffusion, which carries saturation to adjacent spectral locations, starts to determine the lineshape. This effect is most strongly pronounced between turning points.

The amount of saturation progressively increases as the temperature is lowered. It is apparent that the $m_I = -1$ manifold saturates less readily than the nitrogen nuclear quantum number $m_I = +1$ manifold. This is consistent with the idea that the effective T_2 value is shorter for the -1 manifold because of greater anisotropy. Additionally, a small inflection is seen on the high-field side of the central peak, which becomes more apparent as the power increases. This feature is attributed to the X-Y turning point of the $m_I = -1$ manifold. Enhancement of this feature relative to the $m_I = 0$ manifold is attributed to differing amounts of partial saturation of the two manifolds at higher power. In contrast, a strong inflection, which is prominent at low power and temperature, is seen to the low-field side of the central peak. It is attributed to the XY turning point of the $m_I = +1$ manifold. The idea of obtaining spectral information by altering the amount of saturation in the slow tumbling domain is apparent and can be expected to become increasingly useful as the microwave frequency increases.

In another experiment, NARS spectra were collected at a moderately slow sweep rate while slowly increasing the microwave power to investigate saturation behavior across the entire spectrum, and various displays were created by the method of differential saturation [20]. Figure 5A shows raw NARS spectra collected under non-saturating conditions (-32 dB, $\sim P_{1/2}*0.05$), moderately saturating conditions (-20 dB, $\sim P_{1/2}$), and saturating conditions (-8 dB, $\sim P_{1/2}*20$). Comparison of these spectra reveals substantial differences in saturation behavior of each manifold as a result of T_2 effects.

Because each manifold saturates differently, it is possible to separate the manifolds by subtracting spectra collected at two microwave powers as long as rapid passage effects can be avoided. If we have a first spectrum $S(H)_{LP}$ and a second spectrum $S(H)_{HP}$, where LP and HP stand for low power and high power, respectively, then we can artificially form a spectrum of easily saturated features (Eq. 2), $S(H)_{esf}$.

$$S(H)_{esf} = AS(H)_{LP} - S(H)_{HP} \quad (2)$$

Here, A is a constant that is the minimum value that results in an always positive value of $S(H)_{esf}$. This spectrum is easily created and can give insight into the process of motional narrowing of the three nuclear manifolds of an ^{14}N spin label.

Figure 5B shows two spectra collected at microwave powers differing by a factor of six. To account for the change in amplitude due to the increase in microwave power, the spectrum collected at -35 dB was multiplied by $2^{3/2}$. When this scaled spectrum is subtracted from the higher power spectrum, manifolds that are unaffected by power saturation will go to zero. Figure 5C shows that the $m_I = -1$ manifold exhibits no signs of saturation under these conditions, while the $m_I = 0$ and $m_I = +1$ manifolds exhibit moderate saturation effects.

Removal of the high-field manifold through subtraction of a partially saturated spectrum improves the resolution of the high-field portion of the center manifold. If there exists a set of conditions where the $m_I = +1$ manifold can be removed in a similar fashion, it becomes possible to isolate each manifold individually. This method would also be useful in separation of overlapping spectra from multiple species.

3.2 Probing Rapid Passage with Directional Sweeps

Rapid passage phenomena were probed by acquiring the down-field sweep and comparing it to the traditional up-field sweep display. NARS has typically been performed by collecting data on those portions of the triangle where the magnetic field sweep rate is positive, forfeiting the data at the apices of the triangle and when the magnetic field sweep rate is negative. With collection of data on the return sweep, the transfer of saturation within the sweep shifts direction. Comparison of the spectra acquired on the up- and down-sweeps is a way to investigate passage phenomena.

Figure 6 illustrates the difference between NARS spectra recorded on the up- or down-sweep of the triangle at -30°C and high microwave power (~30x greater than $P_{1/2}$). Spectra were aligned using the Hyde and Pilbrow method, which states that the trace of the g-tensor ($g_{iso} = (g_x + g_y + g_z)/3$) can be found where the first moment is zero, *i.e.* the point where the area under the curve is equal on each side [13]. The proof of the theorem assumes that spectra are obtained under non-saturating microwave power conditions. Thus, at non-saturating microwave power levels in the absence of passage effects, the up- and down-sweeps are expected to be identical when aligned in this manner. However, the overlaid spectra in Fig. 6A are slightly offset and have a different line shape, indicating the presence of rapid passage phenomena. These effects are less pronounced at shorter rotational correlation times and at lower microwave powers.

The leading edge of the down-field turning point is sharper than the trailing edge in the up-sweep. When the direction of the sweep is reversed, the up-field turning point is sharper than the down-field turning point. This occurs because the trailing turning points of the sweep are affected by saturation transfer and passage effects while spins excited at the leading edge of the spectrum are unaffected by the relaxation of previously excited spins in the sweep.

When the Hyde and Pilbrow method fails, the difference between the up-sweep and the down-sweep (Fig. 6B) looks somewhat similar to a first harmonic response. This is expected since subtracting two spectra that are offset in field is similar to using MDIFF [9], but the difference in the phase of the $m_I = \pm 1$ turning points as well as the high resolution found in the central manifold indicate a more complex response.

The effect of the magnetic field sweep rate was investigated by holding the triangular frequency constant while incrementally reducing the amplitude of the sweep and collecting data on the up-sweep (Fig. 7). The incident power of 4.1 mW results in strong saturation of the $m_I = 0$ transitions, which saturate more easily at slower magnetic field sweep rates. The $P_{1/2}$ value for the $m_I = 0$ manifold is reduced from 1.0 mW at 260 kG/s to 0.5 mW at 65 kG/s.

Similar lineshapes were observed using magnetic field modulation in early saturation transfer studies [21]. Thomas, Dalton, and Hyde [22] developed the empirical parameter L″/L to characterize slow rotational diffusion, where L″ is the height of the low-field region between turning points, and L is the height of the low-field turning point. It occurs to the authors that this ratio, as seen in Fig. 7 at 260 kG/s sweep rate, could serve a similar purpose. The ratio H″/H for sweeps in the opposite direction might also be used.

In order to identify conditions where alignment using the Hyde and Pilbrow method was valid, experiments were repeated at a slower sweep rate and lower microwave power. Figure 8 shows two instances where the sweep rate and microwave power were sufficient to avoid passage, resulting in nearly identical up-sweep and down-sweep spectra. Interestingly, even at such low powers, a four-fold increase in sweep rate was sufficient to cause the Hyde and Pilbrow method to fail. This suggests that a thorough investigation of incipient passage phenomena may be possible by incrementally altering the field sweep rate at variable microwave power. It follows that saturation behavior of the entire spectrum can be studied by slowly increasing the microwave power and collecting using a very slow magnetic field sweep rate. To the authors' knowledge, this is the first method to provide a systematic approach to separation of passage and saturation phenomena.

The central assumption of NARS spectroscopy as it has been developed [7-9] is that the conditions for non-adiabatic rapid passage are avoided – hence the name non-adiabatic rapid sweep. The display of Fig. 8 provides a means for validation of this assumption. In addition, it may be useful as a means of identifying turning points.

4. Discussion

4.1 NARS CW saturation of spin-labels in the slow tumbling domain

Spin-labels undergoing rotational diffusion in the range of correlation times between 10^{-7} to 10^{-10} s are considered first. Motional narrowing effects are occurring, and the stochastic Liouville theoretical treatment as developed by Freed and colleagues is an appropriate method for spectral analysis under saturating conditions [23, 24]. At the short end of this range of rotational correlation times, the analysis of Hyde, which includes the addition of the Rabi transition probability term to the CW solution of the Bloch equations, provides an introduction to the subject [25]. The work of Robinson, Haas, and Mailer provides a systematic consideration of mechanisms of spin-lattice relaxation of spin labels in the fluid phase [26].

The primary advantage of NARS saturation experiments compared to similar experiments using 100 kHz field modulation is that NARS gathers information at a single spectral point

while the field modulation technique gathers information over the spectral range that is swept by the modulation amplitude. Over a wide range of conditions, it seems that the electron spin-lattice relaxation time does not vary across the spectrum. However the characteristic time for loss of phase coherence provides an effective T_2 value that varies considerably. Comparison of NARS spectra under saturating and non-saturating conditions provides information about the spectral dependence of the effective T_2.

4.2 CW Saturation Experiments in the Very Slow Tumbling Domain

Hyde and Dalton called attention to a special range of conditions that occur when a nitroxide radical spin label undergoes rotational diffusion in the range of correlation times of 10^{-3} to 10^{-7} s [14]. In this range, the spectrum at low microwave powers shows almost no indication of motion and closely resembles the powder spectrum of the nitroxide radical. However, several kinds of experiments at higher microwave powers can be performed that reveal the presence of rotational diffusion in this range. Generally these experiments go under the rubric of “saturation transfer spectroscopy.”

Three kinds of saturation transfer effects can be identified: i) True saturation transfer. Electron-electron double resonance (ELDOR) can be used for observation of this effect. Rotational diffusion carries saturation at one part of the spectrum to other parts of the spectrum. ii) Adiabatic rapid passage effects that are affected by rotational diffusion as pioneered by Hyde and Dalton [14] and reviewed by them [27]. Display of the first harmonic dispersion with the reference phase of the phase-sensitive detector 90° out-of-phase, or, alternatively, the second harmonic absorption again with the reference phase in the out-of-phase position reveals the effects. iii) CW saturation. Because the phase memory time (also sometimes called the “effective T_2”) varies across the spectrum in a manner that depends on the rotational correlation time, so does the CW saturation display even though T_1 seems to show no spectral dependence.

Saturation effects in the very slow tumbling domain have been analyzed by Robinson and co-workers in a series of papers using the method of Gordon and Messenger [28]. Citations are given in the review article of Hyde and Dalton [27]. Physically, one considers rotational diffusion from one solid angle of orientations of the spin label to another solid angle. Spins remain in a solid angle for a sufficiently long time on the time scale of spin lattice relaxation that the effective T_2 can be defined. This time is longer when the solid angle that is defined by the spins under irradiation corresponds to a spectral turning point and shorter when it lies between turning points, resulting in a spectral dependence of CW saturation.

A conclusion of this paper is that differential saturation experiments that are analyzed according to Eq. 2, above, using NARS CW saturation data obtained in the very slow tumbling domain are advantageous compared with data obtained using sinusoidal field modulation with lock-in detection. This is because the constant A (see Eq. 2) can be determined in an objective manner since the spectrum of unsaturated spins must be everywhere positive. Thus, as shown in the Results section, one can set this parameter such that the region between turning points of the nuclear manifold that corresponds to nuclear quantum number -1 has zero intensity. In this manner, the M_Z turning point is clearly defined because it corresponds to unsaturated spins. Also, if desired, one could set the

parameter to a different value to determine the turning points for the manifold that corresponds to nuclear quantum number +1. In addition, since the regions between turning points are observed with intensities that are similar to that of the turning points in the NARS display, comparisons can be made as a function of incident microwave power. These analyses can be performed retrospectively using the same data.

As an example of the spectroscopic benefits of differential saturation, one does not, in general, expect the nitrogen hyperfine tensor to be strictly axial. Preliminary data suggest that differential saturation using NARS saturation data will allow determination of A_X and A_Y using X-band data. This procedure appears to be a general method to obtain precise spectral displays of turning points. The word “precise” is used because the observed spectral data were obtained at low power and are not likely to be affected by passage effects.

One also could ask if differential saturation could lead to a general method to estimate the rotational correlation time. It is suggested here that a ratio of $P_{1/2}$ at a turning point to one in a region between turning points would provide a suitable metric. It may even be possible to characterize slow anisotropic rotational diffusion in this way. However, these ideas are deferred for future studies.

The parameter space for differential saturation NARS experiments includes the specific powers that are presumed to be saturating and non-saturating. This space has not yet been explored systematically in the very slow tumbling domain. The additional parameter of the microwave frequency also has not been explored. Experiments reported here were at X-band. As the microwave frequency increases, the conditions for very slow rotational diffusion become increasingly well satisfied. Motional conditions can exist where some spectral regions are in the very slow tumbling domain and other regions are not. Variation of microwave frequency using differential NARS saturation offers an opportunity to explore these conditions.

4.3 Incipient Passage effect in NARS in the very slow tumbling domain

There are three experimental parameters in the field of EPR adiabatic rapid passage: the microwave power, the magnetic field sweep rate, and the direction of sweep. In CW EPR with magnetic field modulation, the corresponding parameters are microwave power, the amplitude of the sinusoidal magnetic field modulation, and the frequency of modulation. The early NMR paper of Bloch, Hansen and Packard provides photographs of the oscilloscope under various passage conditions that are essentially identical to effects seen in NARS [29]. We have come to understand that all passage effects arise from FID with the rich variability of observable spectra being dependent on experimental parameters and sample relaxation properties [30].

Here we introduce the concept of *incipient* adiabatic rapid passage, (iARP) which is defined as the earliest evidence of free induction decay as the microwave power and magnetic field sweep rate are gradually increased. For a single symmetric EPR line, the iARP is manifested as a slight broadening of the line on the trailing edge of the sweep. The observed line is no longer symmetric. As the sweep rate and microwave power increase, a pattern of oscillations is seen on the trailing edge of the sweep, which is the fully developed FID.

A novel idea of this paper is that iARP effects are more prominent at turning points than between turning points in the very slow tumbling domain because of the difference in effective T_2 values in these regions. Comparison of spectra obtained in the up-sweep portion of the triangular modulation with down-sweep spectra is the most obvious way to detect iARP effects. If the field sweep is centered at a value of H_0 that is set to zero, then up- and down-sweeps can be made to appear similar by a simple reversal of sign of the magnetic field in the digitized spectrum of one or the other – followed by subtraction, see Fig. 8. The difference spectra reveal derivative-like line-shapes at the turning points with nearly complete cancellation between turning points. From the perspective of the spectroscopist, the motivations for iARP and for differential saturation NARS are similar – both reveal the turning points and, in principle, both can give information about slow rotational diffusion.

iARP shifts cause breakdown of the g-value moment theorem of Hyde and Pilbrow [13], as stated earlier. Alignment of the apparent g-value traces prior to subtraction is an objective and suitable procedure for very small shifts. In addition to subtraction of two spectra obtained by sweeping in opposite directions, subtraction of spectra obtained at different field sweep rates is a possible alternative that was not tested here. A mixed display of differential saturation and iARP is also a possible alternative from a practical point-of-view. Simultaneous detection of dispersion and absorption in this context may also be useful. This idea follows naturally from the model of Waring [30].

Subtraction of slightly shifted identical spectra is mathematically identical to the moving difference (MDIFF) method of Hyde et al. [9] for transforming a pure absorption into a derivative-like spectrum. This was found to be a useful tool during the course of the work presented here. We have presented a variety of new methods for spectral analysis in the domain of very slow rotational diffusion of nitroxide spin-labeled biomolecules. They are CW methods that depend on spectral variation of the effective T_2 value in the presence of a modest level of incident microwave power. This variation of T_2 in the case of isotropic rotational diffusion arises from differences in spectral diffusion because of the anisotropy of the nuclear hyperfine and Zeeman interactions. If the rotational diffusion is anisotropic, additional spectral effects are expected. These CW methods can be said to be non-linear. Retrospective transformation of spectra to derivative-like displays, which is a linear process with interesting filter properties, may be convenient.

4.4 Strong passage effects in NARS

Under conditions of faster sweep rate, major changes that depend on sweep direction are seen across the NARS spectrum. Observations made under these conditions are reported here, but the experimental parameter space is large and these effects have not been thoroughly studied. The goal of such studies would be to characterize the anisotropy of rotational diffusion in the very slow tumbling domain.

A particular problem is the use of segmental acquisition in the situation where field sweep outside of the spectral window that is acquired affects the signal in the window. It is hypothesized that this problem could be solved by the use of a trapezoidal sweep where the spin system before each sweep, whether up or down, is allowed to come to equilibrium. Experiments as a function of segmentation width and sweep rate are desirable.

Approximate overall estimates of rotational diffusion using the historic method of second harmonic absorption out-of-phase in combination with reference data from standard samples could be readily duplicated using NARS detection, and the sensitivity of the measurement is expected to be higher. However, the specificity of the historic method may be better since all signal intensity in the out-of-phase condition arises from passage.

Although the method of differential saturation can be expected to be sensitive to overall spin label rotational diffusion, it could also be sensitive to local rotational modes of the tethered spin label. That was a concern in the development of the saturation transfer methodology, but consistency of measurements over a range of samples and viscosities allayed that concern. It should be considered in the development of any new method to study very slow rotational diffusion.

Alignment of up-field and down-field sweeps based on the Hyde and Pilbrow method of moments followed by subtraction [13] is a good way to detect the presence of incipient passage effects. However, it does not have apparent benefit in the case of strong passage effects. It is suggested here that a three dimensional display of up/down difference spectra as a function of the difference interval would provide a better visualization from which metrics of anisotropy of slow rotational diffusion could be extracted.

Acknowledgements

We thank our colleagues and assistants for their helpful comments and discussions. This work was supported by grants EB001980 and EB002052 of the National Institutes of Health.

References

1. Klug CS, Feix JB. Methods and applications of site-directed spin labeling EPR spectroscopy. Methods in cell biology. 2008:617–658. [PubMed: 17964945]
2. Bales BL, Peric M, Lamy-Freund MT. Contributions to the Gaussian line broadening of the proxyl spin probe EPR spectrum due to magnetic-field modulation and unresolved proton hyperfine structure. J. Magn. Reson. 1998; 132:279–286. [PubMed: 9632554]
3. Poole, CP. Interscience. New York, NY: 1967. Electron Spin Resonance: A Comprehenisve Treatment of Experimental Techniques.
4. Fedin M, Gromov I, Schweiger A. Absorption line CW EPR using an amplitude modulated longitudinal field. J. Magn. Reson. 2004; 171:80–89. [PubMed: 15504685]
5. Hyde JS, Strangeway RA, Camenisch TG, Ratke JJ, Froncisz W. W-band frequency-swept EPR. J. Magn. Reson. 2010; 205:93–101. [PubMed: 20462775]
6. Stoner JW, Szymanski D, Eaton SS, Quine RW, Rinard GA, Eaton GR. Direct-detected rapid-scan EPR at 250 MHz. J. Magn. Reson. 2004; 170:127–135. [PubMed: 15324766]
7. Kittell AW, Camenisch TG, Ratke JJ, Sidabras JW, Hyde JS. Detection of undistorted continuous wave (CW) electron paramagnetic resonance (EPR) spectra with non-adiabatic rapid sweep (NARS) of the magnetic field. J. Magn. Reson. 2011; 211:228–233. [PubMed: 21741868]
8. Kittell AW, Hustedt EJ, Hyde JS. Inter-spin distance determination using L-band (1-2 GHz) non-adiabatic rapid sweep electron paramagnetic resonance (NARS EPR). J. Magn. Reson. 2012; 221:51–56. [PubMed: 22750251]
9. Hyde JS, Bennett B, Kittell AW, Kowalski JM, Sidabras JW. Moving difference (MDIFF) non-adiabatic rapid sweep (NARS) EPR of copper(II). J. Magn. Reson. 2013; 236:15–25. [PubMed: 24036469]

10. Altenbach C, Flitsch SL, Khorana HG, Hubbell WL. Structural studies on transmembrane proteins. 2. Spin labeling of bacteriorhodopsin mutants at unique cysteines. Biochemistry. 1989; 28:7806–7812. [PubMed: 2558712]
11. Portis AM. Rapid passage effects in electron spin resonance. Phys. Rev. 1955; 100:1219–1222.
12. Portis, AM. Technical Note 1. Sarah Mellon Scaife Radiation Laboratory, University of Pittsburgh; Pittsburg, PA: 1955. unpublished
13. Hyde JS, Pilbrow JR. A moment method for determining isotropic g values from powder EPR spectra. J. Magn. Reson. 1980; 41
14. Hyde JS, Dalton LA. Very slowly tumbling spin labels: adiabatic rapid passage. Chem. Phys. Lett. 1972; 16:568–572.
15. Beth, AH.; Hustedt, EJ. Saturation transfer EPR: Rotational dynamics of membrane proteins. In: Eaton, SS.; Eaton, GR.; Berliner, LJ., editors. Biological Magnetic Resonance: Biomedical EPR - Part B: Methodology, Instrumentation, and Dynamics. Kluwer, NY: 2005. p. 369-407.
16. Marsh, D.; Horvath, LI.; Pali, T.; Livshits, VA. Saturation transfer spectroscopy of biological membranes. In: Eaton, SS.; Eaton, GR.; Berliner, LJ., editors. Biological Magnetic Resonance: Biomedical EPR - Part B: Methodology, Instrumentation, and Dynamics. Kluwer, NY: 2005. p. 309-367.
17. Weger M. Passage effects in paramagnetic resonance experiments. Bell System Tech. J. 1960; 39:1013–1112.
18. Fleissner MR, Cascio D, Hubbell WL. Structural origin of weakly ordered nitroxide motion in spin-labeled proteins. Prot. Sci. 2009; 18:893–908.
19. Yu YG, Thorgeirsson TE, Shin YK. Topology of an amphiphilic mitochondrial signal sequence in the membrane-inserted state: a spin labeling study. Biochemistry. 1994; 33:14221–14226. [PubMed: 7947833]
20. Livshits VA, Marsh D. Application of the out-of-phase absorption mode to separating overlapping EPR signals with different T1 values. J. Magn. Reson. 2005; 175:317–329. [PubMed: 15946873]
21. Hyde JS, Thomas DD. New EPR methods for the study of very slow motion: application to spin-labeled hemoglobin. Ann. N.Y. Acad. Sci. 1973; 222:680–692. [PubMed: 4361877]
22. Thomas DD, Dalton LA, Hyde JS. Rotational diffusion studied by passage saturation transfer electron paramagnetic resonance. J. Chem. Phys. 1976; 65:3006–3024.
23. Freed JH, Bruno GV, Polnaszek CF. Electron spin resonance line shapes and saturation in the slow motional region. J. Phys. Chem. 1971; 75:3385–3399.
24. Goldman SA, Bruno GV, Freed JH. ESR studies of anisotropic rotational reorientation and slow tumbling in liquid and frozen media. II. Saturation and nonsecular effects. J. Chem. Phys. 1973; 59:3071–3091.
25. Hyde JS. Saturation of the magnetic resonance absorption in dilute inhomogenously broadened systems. Phys. Rev. 1960; 119:1492–1495.
26. Robinson BH, Haas DA, Mailer C. Molecular dynamics in liquids: spin-lattice relaxation of nitroxide spin labels. Science. 1994; 263:490–493. [PubMed: 8290958]
27. Hyde, JS.; Dalton, LA. Saturation-Transfer Spectroscopy. In: Berliner, LJ., editor. Spin Labeling II: Theory and Applications. Academic Press; New York: 1979. p. 1-70.
28. Gordon, RG.; Messenger, T. Magnetic resonance line shapes in slowly tumbling molecules. In: Muus, LT.; Atkins, PW., editors. Electron Spin Relaxation in Liquids. Plenum, NY: 1972. p. 341-381.
29. Bloch F, Hansen WW, Packard M. The nuclear induction experiment. Phys. Rev. 1946; 70:474–485.
30. Waring RK. Classical microscopic model for magnetic resonance including relaxation effects. Phys. Rev. 1962; 125:1218–1226.

Highlights

- NARS saturation experiments are useful for accessibility studies of oxygen with spin-label.
- Difference spectra under partial saturation conditions enhance spectra.
- The presence of incipient free induction decoy (FID) effects is demonstrated.
- Incipient FID effects can be used in saturation transfer experiments.

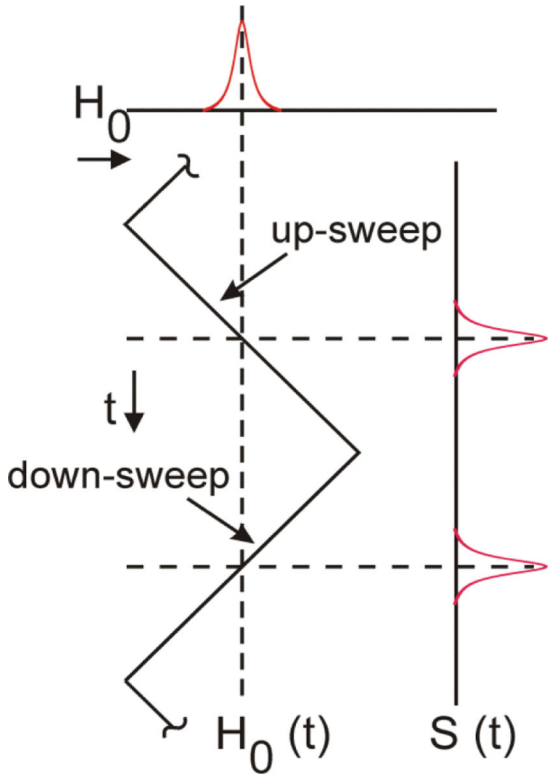

Figure 1.
Rapid passage effects can be investigated using the NARS technique by comparing the ‘up-field sweep’ of the triangle to the ‘down-field sweep’.

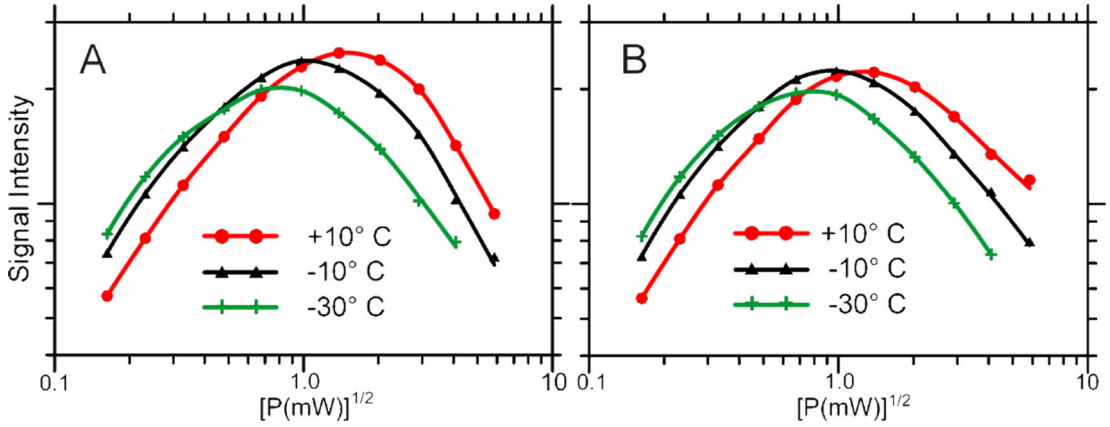

Figure 2.

Power saturation curves of T4L as a function of temperature acquired from the peak-to-peak center line height in spectra recorded with magnetic field modulation (A) and from the center peak height acquired with NARS detection (B); 260 kG/s, up-field sweep.

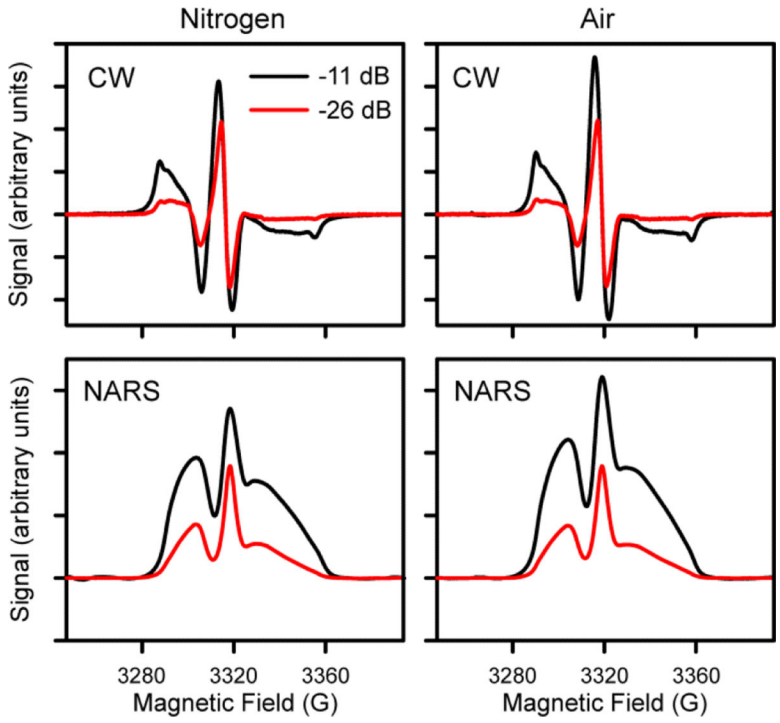

Figure 3.

NARS (up-sweep, 260 kG/s) and CW spectra collected under nitrogen or in the presence of air at 30°C.

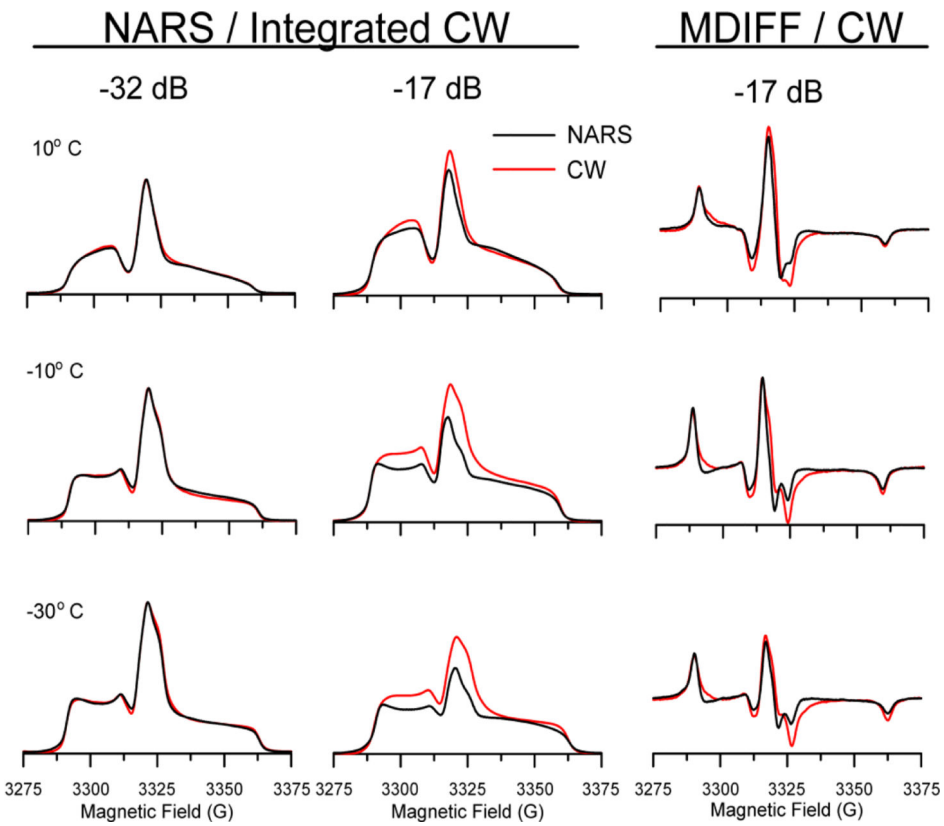

Figure 4.

NARS (black, up-field sweep, 260 kG/s) and CW (red) EPR spectra of T4- Lysozyme under non-saturating (-32 dB, 53 μW) and moderate saturating (-17 dB, 1.9 mW) conditions. Rotational correlation times of 1.7 μs (−30°C), 0.26 μs (−10°C), and 0.077 μs (10°C) were estimated using the Debye expression. Spectra were normalized to the lowest microwave power, as in Fig. 2.

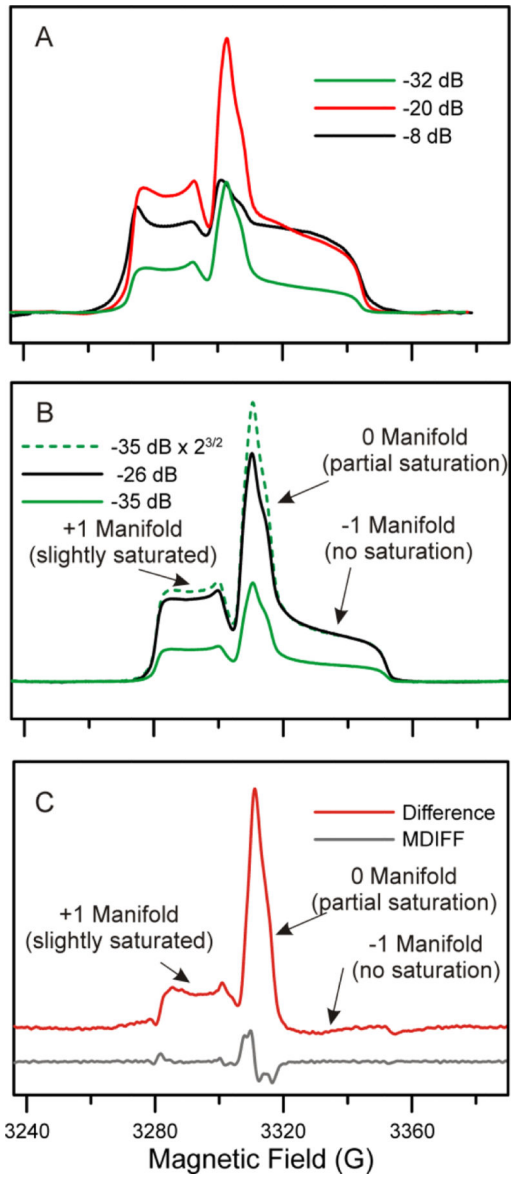

Figure 5.

Resolution enhancement by differential saturation at −10°C (130 kG/s). A) Raw NARS spectra collected under non-saturating (-32 dB), moderate saturating (-20 dB), and saturating conditions (-8 dB). B) NARS spectra collected at two microwave powers, adjusting the amplitude of the lower power to account for the expected amplitude difference due to the change in microwave power (dashed). C) The difference of the black spectrum from the dashed green spectrum in Panel B in shown in red. MDIFF was applied to the red spectrum to enhance turning points in the lower trace.

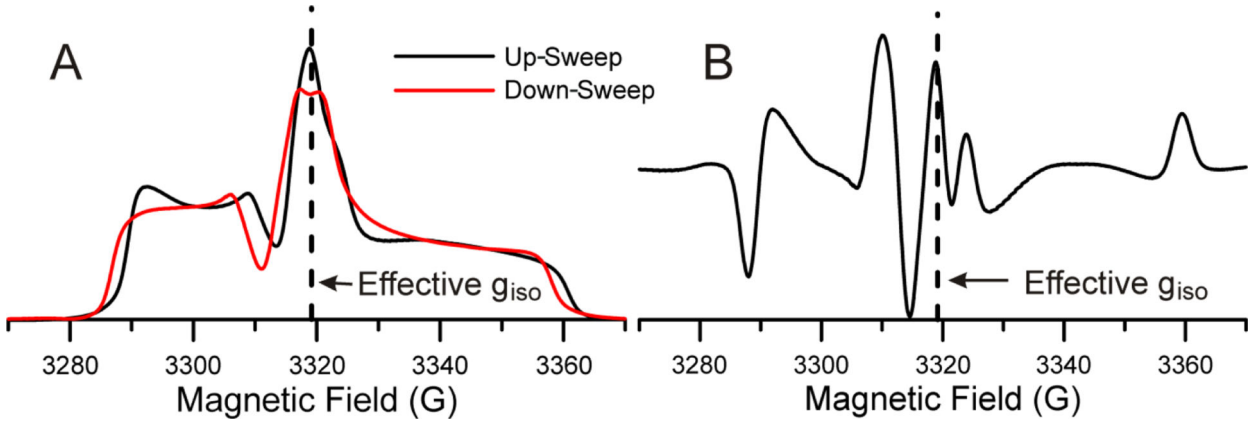

Figure 6.

(A) NARS spectra of T4L acquired on the up- and down-sweeps of the triangle at −30°C with a 260 kG/s sweep rate. Spectra were acquired using powers ~30x greater than $P_{1/2}$, and are aligned using the first moment theorem described by Hyde and Pilbrow [13]. (B) Difference spectrum of the down sweep subtracted from the up sweep.

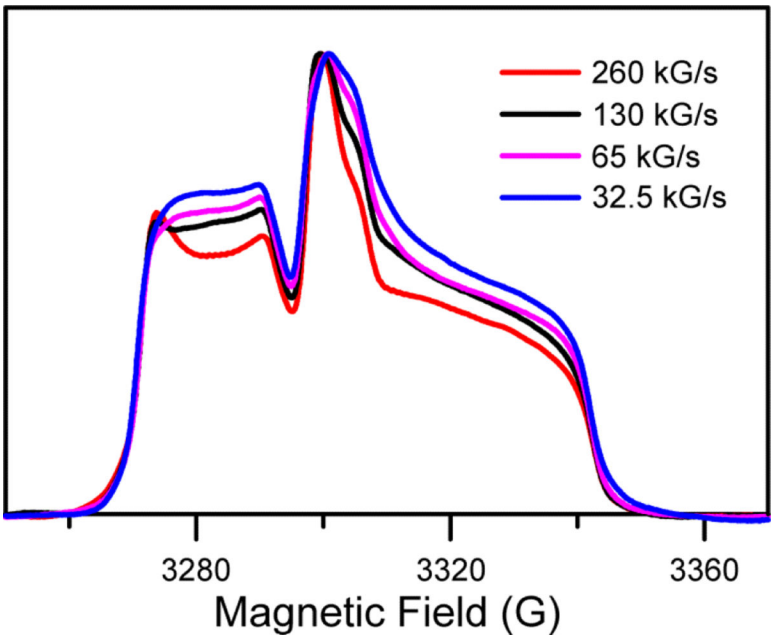

Figure 7.
NARS spectra (up-sweep, normalized to peak) collected at -10°C and 4.1 mW at variable magnetic field sweep rates

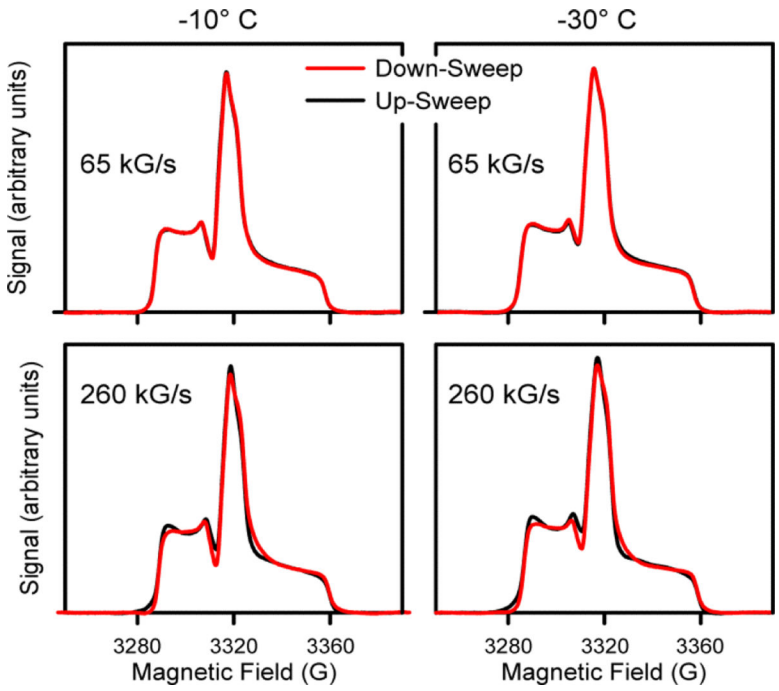

Figure 8.

NARS spectra (26 μW) collected on the upand down-sweep of the triangle at 65 kG/s and 260 kG/s. In the presence of passage effects, the up- and down-sweep will not be identical.